THE JOURNAL OF PHYSICAL CHEMISTRY B

ARTICLE

pubs.acs.org/JPCB

Evaluating the Sensitivity of Lipid Headgroup-Bound Chromophores to Their Local Environment

Iwan Setiawan and G. J. Blanchard*

Department of Chemistry, Michigan State University, East Lansing, Michigan 48824-1322, United States

ABSTRACT: We report on the steady state and time-resolved fluorescence behavior of the chromophore 1,2-dimiryristoyl-*sn*-glycero-3-phosphoethanolamine-*N*-lissamine rhodamine B sulfonyl ammonium salt (SR-DMPE) in a series of solution phase and lipid bilayer environments. The issue of interest is whether or not the lipid headgroup-bound chromophore is sensitive to its local environment under conditions where vesicles have not been formed in lipid-containing mixtures and where unilamellar vesicles have been formed by extrusion. Our data point to the strong interaction of SR-DMPE with 1,2-dimirystoyl-*sn*-glycero-phosphocholine (DMPC) in solution whether or not the solution has undergone extrusion. The amount of SR-DMPE in the lipid-containing systems affects both the steady state and time-resolved spectroscopic response. Excitation of the chromophore to the S_2 state deposits sufficient excess energy into the system to influence its rotational diffusion dynamics, demonstrating significant interactions between SR-DMPE and DMPC. Comparison of SR-DMPE reorientation dynamics in DMPC-containing solutions with corresponding data on SR-DMPE in aqueous solution indicates that the lipids impose a restrictive local environment on the chromophore that is a factor of ca. 10 more viscous than an aqueous environment. The similarity of the reorientation data in all DMPC-containing solutions suggests that SR-DMPE is a local probe that is not sensitive to longer range organization.

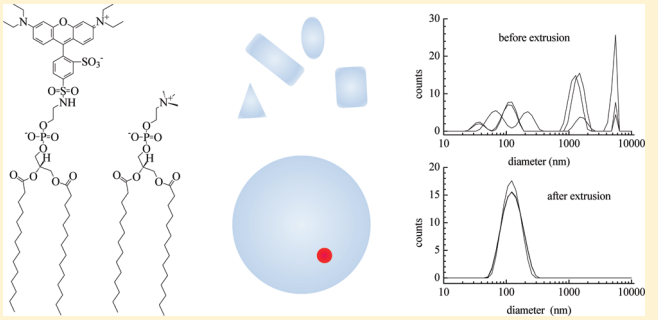

INTRODUCTION

Understanding organization and dynamics within lipid bilayer structures, both free-standing and supported, is a critical issue for both fundamental and practical reasons. Despite the extensive literature extant on lipid bilayer organization and dynamics,[1−29] there remains to emerge a clear understanding of the compositional and organizational requirements for lipid bilayers to support transmembrane proteins in their active forms. The local organization of lipid bilayer constituents around transmembrane proteins is thought to mediate the folding and function of the protein, and the ability to replicate this local organization in systems that do not incorporate the full compositional complexity of mammalian plasma membranes stands as a limitation to the ability to create biomimetic structures capable of functioning as chemical sensors. A prerequisite for understanding this complex issue is determining which factors are important in mediating organization in simple model systems.

There are a number of ways to interrogate lipid bilayer structures, depending on their structural format. Supported bilayers are amenable to electrochemical interrogation if the solid support is conductive. For free-standing bilayer structures such as unilamellar vesicles, electrochemical characterization is not possible, but spectroscopic methods are capable of providing significant insight into local organization.[30−37] NMR[38−40] and neutron scattering[41] studies have proven invaluable, for example, in elucidating the details of phase transitions and intermolecular interactions in bilayer structures. One advantage of NMR studies is that they do not require the incorporation of a structurally perturbative probe into the bilayer. Optical spectroscopic methods have seen wide use in the study of lipid bilayer systems. While such studies involve the addition of probe(s) to the bilayer, for sufficiently low chromophore concentrations the perturbation they induce is negligible,[36] allowing the useful examination of the bilayer structure by these methods.

The Blanchard group has utilized time-resolved optical spectroscopic techniques to interrogate local organization and dynamics in bilayer structures.[32−37] When performing such experiments, a free probe can either partition into the nonpolar lipid bilayer region or it can be tethered to a bilayer constituent. For the former class of experiments, success relies on the chromophore locating exclusively within the lipid acyl chain region, but in that area further localization is not achievable. Even with this limitation, such probes have proven to be very useful in elucidating phase transitions in lipid bilayer systems.[36]

Using a tethered chromophore as an optical probe affords exquisite control over the location of the probe in the bilayer. Typically, chromophores are bound to phospholipids either at the end of one of the acyl chains or to the phospholipid headgroup. For polar tethered chromophores, localization of the chromophore within the acyl chain region is questionable,

Received: October 7, 2011
Revised: December 12, 2011
Published: December 16, 2011

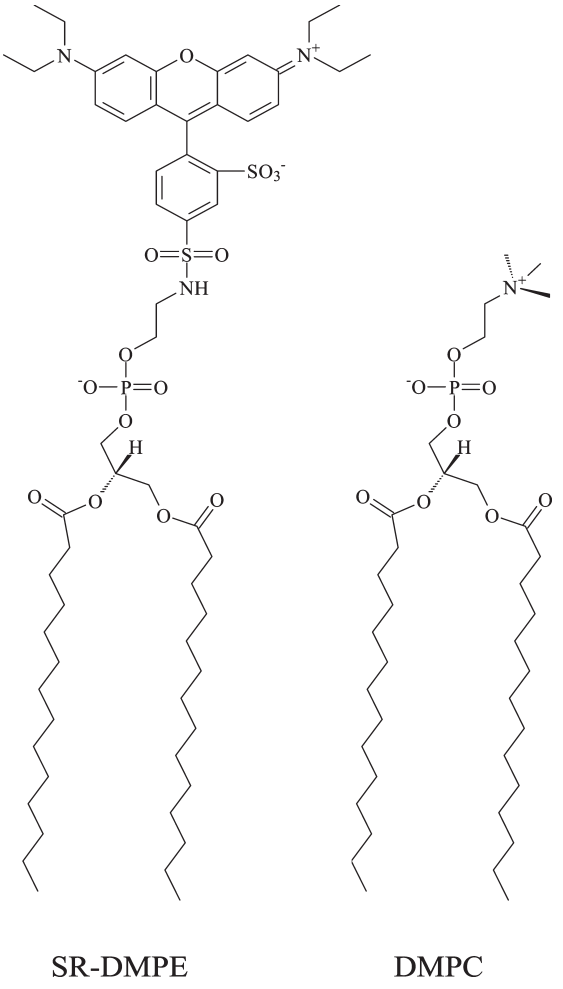

Figure 1. Structures of SR-DMPE (left) and DMPC (right).

and conformational changes in the tethering acyl chain can allow the chromophore to reside in the vicinity of the lipid polar headgroup. For polar headgroup-tethered chromophores, interactions between the chromophore and the aqueous region in contact the lipid head groups are sensed. Despite the localization afforded by tethering, there remain substantial questions about the location of the probe within bilayer structures and the sensitivity of the tethered probe to its local environment.

In an attempt to address these questions, we have used the probe 1,2-dimiryristoyl-*sn*-glycero-3-phosphoethanolamine-*N*-lissamine rhodamine B sulfonyl ammonium salt (SR-DMPE, Figure 1) in a series of solutions to understand the response of the tethered chromophore as a function of solution composition and morphology. We have studied the steady state spectroscopy and rotational diffusion dynamics of SR-DMPE in aqueous solutions and buffered aqueous solutions as well as in solutions containing DMPC, both prior to and after extrusion to form unilamellar vesicles. The information we report demonstrates the sensitivity and limitations of this type of chromophore in terms of reporting on its local environment.

EXPERIMENTAL SECTION

Materials Used and Vesicle Preparation. DMPC (1,2-dimyristoyl-*sn*-glycero-3-phosphocholine) and SR-DMPE (1,2-dimyristoyl-*sn*-glycero-3-phosphoethanolamine-*N*-lissamine rhodamine B sulfonyl ammonium salt) (Figure 1) were purchased from Avanti Polar Lipids and used as received. Lipid-containing solutions were prepared by evaporating chloroform solvent from the lipid mixture and hydrating the resulting dry lipid with Trizma (Tris) -HCl buffer (Sigma-Aldrich, St. Louis, MO). Trizma buffer (10 mM, pH 7.7) was prepared using water from a Milli-Q Plus water purification system (Millipore, Bedford, MA). For lipid-containing samples, the concentration of DMPC was 1.5 mM with SR-DMPE concentrations of 0.1 mol % (1.5×10^{-6} M) and 0.01 mol % (1.5×10^{-7} M). For buffered and unbuffered aqueous SR-DMPE solutions, chromophore concentrations of 10^{-6} and 10^{-7} M were used. All aqueous and buffered SR-DMPE solutions were processed five times through a freeze−thaw-vortex cycle to ensure mixing of the sample matrix equivalent to that performed on the lipid-containing solutions. Each cycle consisted of immersion in N_2(l) for 5 min, followed by immersion in a 60 °C water bath for 5 min, then vortexing the thawed sample for 2 min. The hydrated lipid mixtures were either used as hydrated and mixed or were extruded eleven times through a polycarbonate membrane with a nominal pore diameter of 100 nm (Avanti Polar Lipids Inc., Alabaster, AL). All extrusions were performed at room temperature.

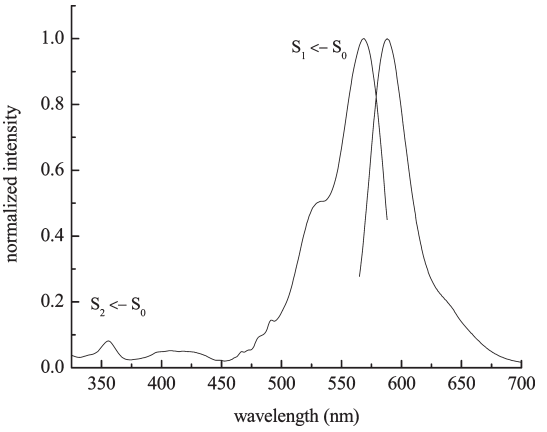

Figure 2. Normalized excitation and emission spectra of 1.5×10^{-6} M SR-DMPE in extruded DMPC.

Steady State Measurements. Steady state excitation and emission spectra were measured using a Spex Fluorolog 3 emission spectrometer. The spectral resolution for both the excitation and collection monochromators was set to 3 nm for all measurements. Emission spectra were acquired for excitation of the SR-DMPE samples at 565 nm. We report the normalized excitation and emission spectra in Figure 2.

Dynamic Light Scattering Measurements. Dynamic light scattering measurements were performed using a Malvern Zetasizer instrument fitted with a HeNe laser (632.8 nm). The concentration of DMPC for both pre- and postextrusion samples was 1 mg of lipid/mL of solution, similar to the concentration used for the time-resolved measurements. The sample temperature for all measurements was 24 °C.

Time-Correlated Single-Photon Counting. Fluorescence anisotropy decay data were collected using a time-correlated single photon counting instrument. This spectrometer has been described previously[42] and we recap its salient features here. The light source is a CW mode-locked Nd:YVO_4 laser that produces 1064 nm pulses (13 ps fwhm) at 80 MHz repetition rate (Spectra Physics Vanguard). The 1064 nm light is frequency doubled and

tripled to produce 2.5 W average power at 355 and 532 nm, with the same pulse duration and repetition rate as the fundamental. The second and third harmonic outputs of the Nd:YVO_4 laser are used to excite cavity-dumped dye lasers (Coherent 702−2). The outputs of these lasers are characterized by ≤5 ps pulses over the spectral range of 430−550 nm (355 nm excitation) and 550 nm −850 nm (532 nm excitation). The repetition rate of the laser is adjustable between 80 kHz and 80 MHz using Gooch and Housego cavity dumping electronics (4 MHz dumping rate was used in these experiments). For the experiments reported here, the dye used to excite the SR-DMPE $S_1 \leftarrow S_0$ transition is Pyromethene 567 (Exciton), operating at 565 nm. For excitation of the SR-DMPE $S_2 \leftarrow S_0$ transition at 350 nm, the dye laser is operated with LDS 698 dye (Exciton) at 700 nm and the output of this dye laser is frequency doubled using a type I $LiIO_3$ SHG crystal. The fundamental output from the dye laser is split, with one portion directed to a photodiode that generates a reference signal, and the other portion directed to the sample. The excitation pulse is polarized vertically for both excitation wavelengths and the power incident upon the sample is 1 mW or less average power for all measurements. Emission from the sample is collected using a 40x reflecting microscope objective (Ealing). The collected emission is separated into polarization components parallel and perpendicular to that of the vertically polarized excitation pulse using a polarizing cube beam splitter. The parallel and perpendicular polarized signal components are detected simultaneously using Spectral Products CM-112 subtractive double monochromators, each equipped with a Hamamatsu R3809U-50 microchannel plate photomultiplier (MCP-PMT) detector. The detection electronics (Becker & Hickl SPC-132) resolve the parallel and perpendicular transients separately, yielding *ca.* 30 ps response functions for each detection channel. The detection electronics include a time-to-amplitude converter (TAC) and a constant fraction discriminator (CFD) that temporally resolves the fluorescence signal for each polarization component. Data are collected using multichannel analyzers that are integral components of the SPC-132 electronics. Data acquisition, detector bias and collection wavelength are controlled using a program written in-house using National Instruments LabVIEW software on a PC.

RESULTS AND DISCUSSION

The use of tethered chromophores to probe local organization and dynamics in confined or organized environments is well established, both experimentally and theoretically. The primary motivation for the use of tethered probes is to control their location within the system. The location of the probe and its effect on the environment it is intended to interrogate is a matter that invariably remains open to question at some level, and we are interested in addressing these issues experimentally. We have chosen to examine the tethered probe SR-DMPE. The chromophore is a rhodamine and its spectroscopic behavior is well understood.[43] The system we intend to probe with this chromophore is the phospholipid DMPC, under conditions where the lipid containing solution has either been processed to form vesicles or prior to such processing. We use steady state and time-resolved fluorescence measurements to interrogate local organization in these systems as a function of solution processing, chromophore concentration and the state to which the chromophore is excited. We consider first the chromophore concentration dependence on the steady state emission properties.

The emission spectrum of SR-DMPE exhibits a concentration-dependence in all of the environments we have examined in this work. We show in Figures 3 and 4 the emission spectra of SR-DMPE as a function of concentration in the media examined here.

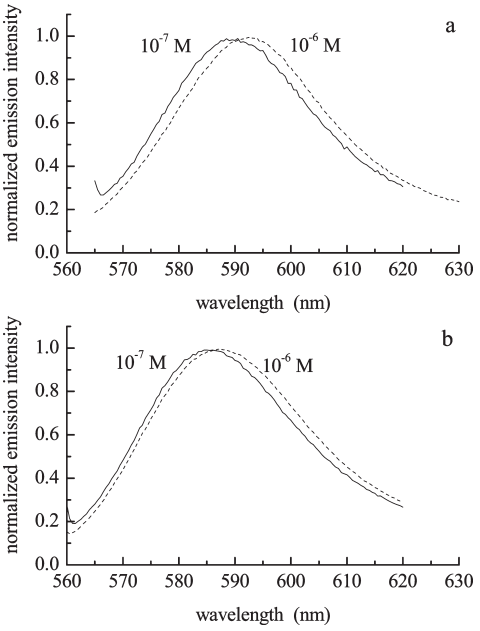

Figure 3. (a) Normalized emission spectra of 10^{-6} M (dashed line) and 10^{-7} M (solid line) SR-DMPE in aqueous solution. (b) Normalized emission spectra of 10^{-6} M (dashed line) and 10^{-7} M (solid line) SR-DMPE in Trizma-buffered aqueous solution at pH 7.7.

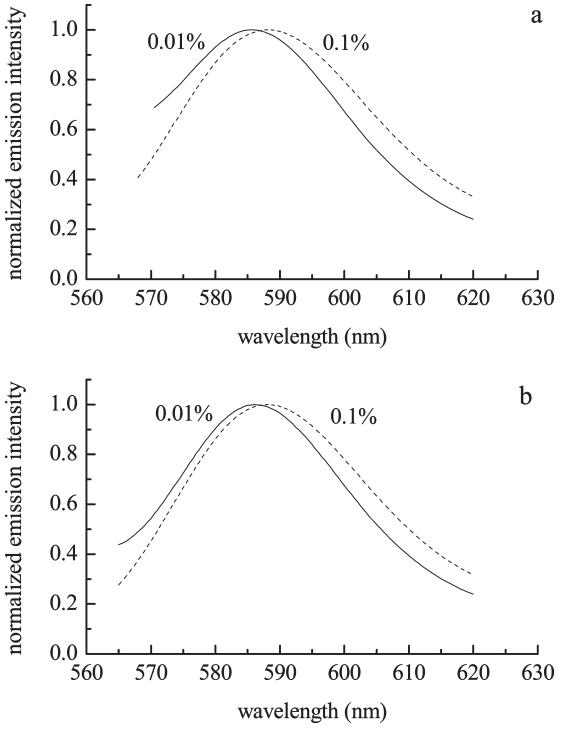

Figure 4. (a) Normalized emission spectra of 0.1 (dashed line) and 0.01 mol % (solid line) SR-DMPE in a 1.5 mM DMPC buffered solution prior to extrusion. (b) Normalized emission spectra of 0.1 (dashed line) and 0.01 mol % (solid line) SR-DMPE in a 1.5 mM DMPC buffered solution after extrusion to form 100 nm diameter vesicles.

In Figure 3a, the normalized emission spectrum of SR-DMPE in water exhibits a red shift of the maximum from 590 to 593 nm with a change in concentration from 10^{-7} to 10^{-6} M. For SR-DMPE in aqueous Trizma buffer at pH 7.7, the spectral shift from 586 to 588 nm is similar in magnitude, but examination of these data suggests that the concentration-dependent spectral shift seen in Trizma buffer solution is slightly smaller than it is in water. The difference in spectral shifts for these two sets of data is not clearly resolved, but the fact that the water and buffered aqueous solutions are characterized by different ionic strength may account in part for any subtle difference between the two sets of data. The fact that a spectral red shift is seen for SR-DMPE with increasing concentration indicates that there are chromophore−chromophore interactions occurring at the higher probe concentration. This is perhaps not surprising due to the amphiphilic nature of the probe and the likelihood of nonpolar interactions between acyl chain moieties in an aqueous environment.

We understand these spectral shifts for rhodamine in the following manner. For the spectral red shifts seen with increasing chromophore concentration, the interactions between chromophores serve to stabilize the S_1 state, possibly through $\pi^*-\pi$ interactions. The spectral blue-shifts seen with increased solution ionic strength suggest that some interaction between either the buffer ions and the chromophore or the buffer ions and the lipid headgroups stabilize the chromophore S_0 state to a greater extent than the S_1 state. This effect cannot be simply a stabilization of the permanent dipole moment in the two states because the S_1 dipole moment for rhodamines is expected to be larger than that for the S_0 state. Further work with aqueous solutions containing different ionic species over a range of concentrations will be required to resolve the detailed mechanism(s) of the spectral shifts we observe.

It is useful to note that if the chromophore were distributed homogeneously in solution, the average distance between SR-DMPE molecules would be 1.47×10^{-5} cm for a 10^{-6} M solution and 3.17×10^{-5} cm for a 10^{-7} M solution. We calculate the diffusion coefficient for SR-DMPE to be 3.4×10^{-6} cm^2/s using the Stokes−Einstein equation, implying an average time between collisions between two SR-DMPE molecules of 16 μs for a 10^{-6} M solution and 74 μs for a 10^{-7} M solution. Both of these times are long relative to the fluorescence lifetime of the chromophore (ca. 1.5 ns for SR-DMPE in aqueous solution and 3 ns for SR-DMPE in lipid-containing solution), so the observation of the spectral shift implies that the average duration of chromophore−chromophore interaction must lie between 16 and 74 μs. Without explicit knowledge of the spectral profile of the interacting moiety it is not possible to estimate the interaction time more closely. The observation of a factor of 2 difference in the fluorescence lifetime of SR-DMPE in the two solutions points to the importance of interactions between the chromophore and DMPC in solution. It is typically the case that a chromophore will exhibit a shorter lifetime in a polar environment than in a nonpolar environment. These lifetime data, in conjunction with the anisotropy decay data (vide infra) point to the SR-DMPE probe interacting significantly with DMPC when it is present in solution.

The concentration-dependence of the SR-DMPE fluorescence spectral response is similar for DMPC-containing systems, both prior to and following extrusion to form unilamellar vesicles. We show in Figures 4 these emission spectra. For both systems, the emission maximum shifts from 586 nm for 0.01 mol % (1.5×10^{-7} M) SR-DMPE to 588 nm for 0.1 mol % SR-DMPE (1.5×10^{-6} M). These data are consistent with those for the aqueous solutions, revealing what appears to be qualitatively the same concentration-dependence. The diffusion coefficient for C_{14} tagged lipids in bilayers is $\sim 2 \times 10^{-8}$ cm^2/s,[37] significantly slower than the solution phase translational diffusion coefficient. For 0.01 mol % SR-DMPE in vesicles, the average time between collisions is 613 μs and for 0.1 mol % SR-DMPE this time is 56 μs. The observation of chromophore−chromophore interactions in vesicle systems is thus not surprising. What is significant is that the spectral shift seen for the extruded system is essentially identical to that seen for the nonextruded system. The clear implication of these findings is that the average distance between chromophores is similar, regardless of whether or not vesicles have been formed deliberately. Given the apparent similarity of the steady state emission data for the extruded and nonextruded mixtures, it is important to understand whether or not this similarity persists over the length scales sensed by rotational diffusion measurements.

We have examined the fluorescence anisotropy decay data of SR-DMPE in aqueous and buffered solution and in solutions containing DMPC, before and after extrusion. Dynamic light scattering data Figure 5 demonstrate that the morphologies of the pre- and postextrusion DMPC solutions are very different. In addition to going from a multimodal distribution pre-extrusion to a unimodal distribution postextrusion, there is also a substantial difference in the uniformity of the solutions. The data for three separate measurements are shown in Figure 5. For the pre-extruded solution Figure 5a there are clear differences between measurements and for the extruded solution Figure 5b the DLS

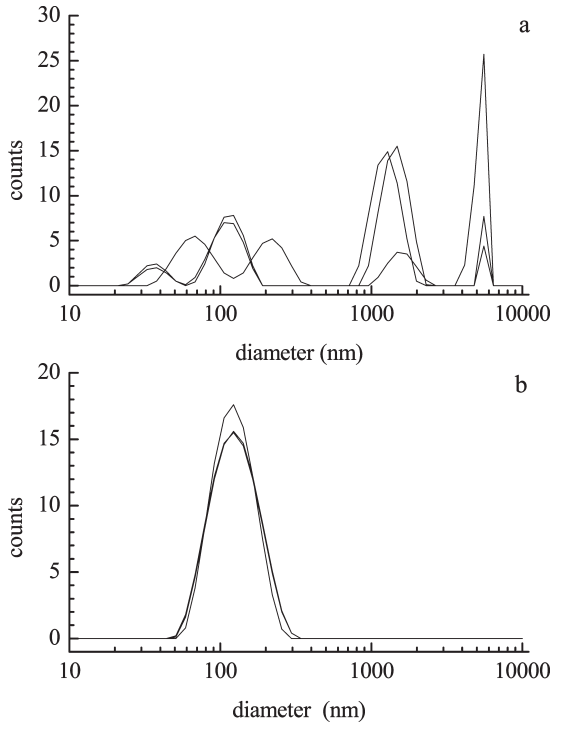

Figure 5. Dynamic light scattering data indicating the size distribution of DMPC structures in solution, (a) prior to extrusion and (b) following extrusion through 100 nm diameter pores. Data for three measurements are presented. Note the reproducibility for the extruded and the measurement to measurement variation exhibited by the sample prior to extrusion.

profiles are identical for each of the measurements. This is not surprising given the inherently heterogeneous nature of these solutions. Given the difference in the pre- and postextrusion samples, it is reasonable to question whether or not the SR-DMPE will occupy similar environments in the two systems. To address this issue, we have examined the dynamics of SR-DMPE in these solutions.

Rotational diffusion is measured through the induced orientational anisotropy function, R(t), which is the normalized difference between emission transients polarized parallel and perpendicular to the incident vertically polarized excitation pulse.

$$R(t) = \frac{I_{\parallel}(t) - I_{\perp}(t)}{I_{\parallel}(t) + 2I_{\perp}(t)} \quad (1)$$

The functional form of the anisotropy decay data depends on the system under investigation; the aqueous solution phase data show that SR-DMPE reorients as a free rotor and in solutions containing DMPC, SR-DMPE produces anisotropy decay data consistent with the chromophore being tethered, a condition treated in the context of the hindered rotor model. The functional form of the anisotropy decay data for the nonextruded DMPC-containing solutions provides insight into local organization around the chromophore. Our data reveal a nonzero infinite-time anisotropy for both pre- and postextrusion solutions, pointing to the existence of substantial spontaneous lipid organization prior to extrusion. This finding is consistent with the presence of aggregated lipids prior to solution processing Figure 5a. We consider the aqueous solution anisotropy data first, to provide a frame of reference for the interpretation of data on lipid-containing solutions.

The chemical information of interest is contained in the functional form of $R(t)$. The anisotropy decay can contain up to five exponential decays, but for most systems only one decay component is recovered. Chuang and Eisenthal have related the anisotropy decay time constants to the Cartesian components of the rotational diffusion constant, and the orientation(s) of the excited and emitting transition dipole moments.[44] For the rhodamine chromophore used in this work, excitation of the long-axis polarized $S_1 \leftarrow S_0$ transition yields $R(t)$ decays with either one or two exponential decay components depending on the shape of the ellipsoid swept out by the reorienting moiety[43]

$$R(t) = 0.4\exp(-6D_z t) \quad \text{(prolate)} \quad (2)$$

$$R(t) = 0.1\exp(-(2D_x + 4D_z)t) + 0.3\exp(-6D_x t) \quad \text{(oblate)} \quad (3)$$

and for excitation of the short-axis polarized $S_2 \leftarrow S_0$ transition, $R(t)$ is given by[43]

$$R(t) = -0.2\exp(-6D_z t) \quad \text{(prolate)} \quad (4)$$

$$R(t) = 0.1\exp(-6D_z t) - 0.3\exp(-(2D_x + 4D_z)t) \quad \text{(oblate)} \quad (5)$$

The Cartesian components D_x, D_y, and D_z can be used to estimate the value of D, depending on the assumed rotor shape and the aspect ratio of the ellipsoid of rotation. The rotor shape information is useful in its own right, but it is also important in relating the experimental data to the physical properties of the surrounding medium. The model used most widely for this purpose is the modified Debye–Stokes–Einstein (DSE) equation (eq 6).[45−48]

$$\tau_{OR} = \frac{1}{6D} = \frac{\eta V f}{k_B T S} \quad (6)$$

The quantity τ_{OR} is the orientational relaxation time constant, obtained from experimental $R(t)$ data. In cases where $R(t)$ contains multiple exponential decays, the Cartesian components of D are determined (eqs 2-5) and used to calculate $D = {}^1/_3(D_x + D_y + D_z)$.[44] The solvent bulk viscosity is given by η, V is the solute hydrodynamic volume, f is a term to account for the solvent–solute frictional interactions, and S is a shape factor that describes the ellipsoidal rotor shape of the probe.[47,48] The model was derived originally for a spherical solute reorienting in a continuum solvent where the f and S terms were not included. Subsequent addition of S and f to the model has brought the DSE model into generally good correspondence with experimental observations, especially for systems where the hydrodynamic volume of the solute is substantially larger than that of the solvent molecules. The theoretical treatment of the term $f\,(0 \le f \le 1)$ has been effective in broadening the applicability of the DSE model to both polar and nonpolar systems.[46]

We have used the Chuang and Eisenthal equations and the DSE model to interpret our experimental data for SR-DMPE in aqueous solution, both with and without Trizma buffer. We calculate the hydrodynamic volume of SR-DMPE to be 1120 Å^3,[49] and take the solvent viscosity to be 1 cP. Using these quantities in eq 6, the modified DSE model predicts $\tau_{OR} = 277$ ps at 20 °C. This calculation assumes $S = 1$ (spheroidal shape) and $f = 1$. Because of the structural complexity of the probe molecule (Figure 1) and the fact that the probe is in a polar environment, it is not unreasonable to expect that the lipid acyl chains would assume a spheroidal shape in solution. The time constant of $\tau_{OR} = 277$ ps is in excellent agreement with the experimental data on SR-DMPE in aqueous solution (Table 1). We note that the experimental time constants appear to be slightly longer for 10^{-6} M solutions than for 10^{-7} M solutions, but these data are not statistically different from one another. If there is an unresolved, slight difference between the 10^{-6} M and 10^{-7} M SR-DMPE solutions, it would correlate with the slight spectral differences seen in Figures 2 and 3. We can conclude from these data that SR-DMPE in aqueous solution exhibits predictable reorientation dynamics and these data provide a useful frame of reference when considering the anisotropy decay data for DMPC-containing systems.

We consider next the SR-DMPE anisotropy decay data for solutions containing DMPC, prior to and after extrusion (Figure 6). It is important to consider that, at least for the case of extruded solutions and possibly for nonextruded solutions as well, the functional form of the anisotropy decay data will be different than the data for SR-DMPE in aqueous solution. Specifically, the headgroup-bound chromophore may be constrained in its motion due to its incorporation into local lipid organization.

Table 1. Reorientation Time Constants for 10^{-6} and 10^{-7} M SR-DMPE in H_2O and Aqueous Trizma Buffer Solution (pH 7.7)

	H_2O	aqueous trizma buffer pH = 7.7
[SR-DMPE] (M)	τ_{OR} (ps)	τ_{OR} (ps)
10^{-6}	319 ± 15	324 ± 22
10^{-7}	286 ± 19	290 ± 20

Constrained rotational motion is treated in the context of the hindered rotor model, where the anisotropy decay function is described by eq 7[50]

$$R(t) = R(\infty) + (R(0) - R(\infty)) \exp(-t/\tau_{HR}) \quad (7)$$

The terms $R(0)$ and $R(\infty)$ are the zero- and infinite-time anisotropies, respectively, and the term τ_{HR} is the hindered rotor decay time constant. In this model the rotational motion of the chromophore is restricted to a conic volume of angle θ_0 and it can execute rotation motion about its tethering bond, described by the wobbling diffusion coefficient, D_w. τ_{HR} is related to these quantities through eq 8[50]

$$\tau_{HR} = \frac{7\theta_0^2}{24D_w} \quad (8)$$

The quantities of interest are θ_0 and D_w, and they cannot be determined uniquely by measurement of τ_{HR} alone. The confining cone angle is related to the zero and infinite-time anisotropies according to eq 9[50]

$$\left[\frac{R(\infty)}{R(0)}\right]^{1/2} = 0.5(\cos\theta_0(1 + \cos\theta_0)) \quad (9)$$

and with the evaluation of the cone angle using the zero- and infinite-time anisotropies, D_w can be determined from the τ_{HR} data. While the physical meaning of D_w is not the same as D, owing to the different physical constraints that operate on the two different diffusion coefficients, system-dependent changes in D_w are reflective of changes in the chromophore local environment.

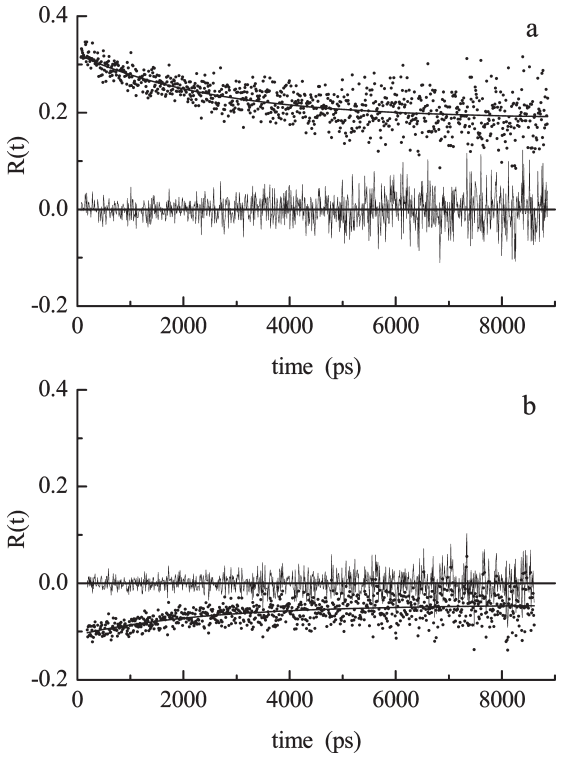

Figure 6. Typical experimental anisotropy decay function for SR-DMPE in DMPC containing solution, following extrusion. (a) Excitation of the $S_1 \leftarrow S_0$ transition, (b) excitation of the $S_2 \leftarrow S_0$ transition. The solid lines are the best fit decays for these data, and the residuals of the fits are shown in each plot.

We address two issues with the data for SR-DMPE in DMPC-containing solutions. The first is the question of whether or not the extrusion of the sample to form unilamellar vesicles gives rise to any discernible change in the dynamics of the rhodamine chromophore. While it is clear from the DLS data (Figure 5) that substantial morphological changes are associated with the extrusion process, it is not clear if these changes are reflected in the local environment of the chromophore. The data presented in Table 2 provide detailed information on the SR-DMPE chromophore dynamics in these environments. Analogous to what is seen in the steady state emission data, there is a chromophore concentration dependence of the dynamic response for these systems. While it is tempting to compare the τ_{HR} data for these solutions, such information can be misleading because τ_{HR} is related to both D_w, the wobbling diffusion coefficient and θ_0 the confining cone angle (eq 8). It is θ_0 and D_w that are related to the local organization of the lipid-containing systems.

We first examine the 0.01 mol % SR-DMPE data for systems prior to and following extrusion. We start with these data based on the assumption that the lower concentration of probe will be less disruptive to the organization of the lipid system. For excitation of the $S_1 \leftarrow S_0$ transition, the values of D_w and θ_0 are the same to within their experimental uncertainty for extruded

Table 2. Data for SR-DMPE Anisotropy Decay in Solutions Containing DMPC, Prior to and Following Extrusion

	0.01 mol % SR-DMPE		0.1 mol % SR-DMPE	
	$S_1 \leftarrow S_0$	$S_2 \leftarrow S_0$	$S_1 \leftarrow S_0$	$S_2 \leftarrow S_0$
		Extruded		
τ_{HR} (ps)	3755 ± 497	1911 ± 147	2785 ± 271	2553 ± 259
$R(0)$	0.32 ± 0.01	−0.12 ± 0.01	0.32 ± 0.01	−0.10 ± 0.01
$R(\infty)$	0.22 ± 0.02	−0.08 ± 0.01	0.19 ± 0.01	−0.04 ± 0.01
D_w (MHz)	18 ± 6	43 ± 16	35 ± 4	63 ± 16
θ_0 (deg.)	28 ± 4	30 ± 5	33 ± 1	43 ± 5
		Non-Extruded		
τ_{HR} (ps)	3388 ± 225	1580 ± 300	2719 ± 160	2819 ± 243
$R(0)$	0.28 ± 0.01	−0.10 ± 0.01	0.31 ± 0.01	−0.08 ± 0.01
$R(\infty)$	0.18 ± 0.01	−0.06 ± 0.01	0.18 ± 0.01	−0.03 ± 0.01
D_w (MHz)	25 ± 5	55 ± 28	38 ± 4	72 ± 13
θ_0 (deg.)	31 ± 3	31 ± 8	34 ± 2	48 ± 4

dx.doi.org/10.1021/jp209651f |J. Phys. Chem. B 2012, 116, 966–973

and nonextruded systems. This finding is significant because it implies that, regardless of whether or not the lipid system has been organized into a unilamellar vesicle, the SR-DMPE chromophore samples effectively the same local environment. Thus the probe is associated with lipids regardless of solution processing, and whatever associated lipid structure exists in these systems (Figure 5) is sufficiently large to render the response of the probe insensitive to such differences.

An examination of the 0.1 mol % data for $S_1 \leftarrow S_0$ excitation provides the same result; D_w and θ_0 are the same for pre- and postextrusion systems. This is not surprising, nor is the result that the D_w values are faster for the higher probe concentration. We assert that the faster chromophore D_w values for higher concentration are reflective of greater disruption of local organization in the lipid structures, likely due to steric and/or charge effects. It is interesting that the values of θ_0 are the same for the two probe concentrations to within the experimental uncertainty. This is likely due to the fact that the probe acyl chains are incorporated in essentially the same lipid environment regardless of the probe concentration, and the headgroup-attached chromophore is sensing disorder in the polar headgroup region.

We have also studied the excitation energy dependence of SR-DMPE dynamics. We have performed these studies to evaluate the effect of excess energy on the lipid local environment. Excitation of the $S_1 \leftarrow S_0$ transition results in the deposition of relatively little excess energy into the bath surrounding the chromophore because emission is from the S_1 state and the rhodamine chromophore has a relatively high fluorescence quantum yield. Excitation to the S_2 state results in the rapid deposition of energy into the chromophore bath because of the rapid nonradiative decay from the S_2 to S_1 manifold. For our measurements, the excess energy is 1.348 eV. We have reported previously on the state-dependent anisotropy decay dynamics for rhodamine 640 in alcohols.[43] The excess energy deposited by $S_2 \rightarrow S_1$ nonradiative relaxation heats the immediate environment of the chromophore, resulting in what can be treated as a decrease in local viscosity. In a previous report on the dissipation of excess energy in a rhodamine chromophore, we found, qualitatively, the same results as we report here.[43] Specifically, the reorientation time of the chromophore is seen to be faster for S_2 excitation than for S_1 excitation. While this trend is not clear from the τ_{HR} data, the D_w data show plainly a factor of ca. 2 increase on going from S_1 to S_2 excitation. In the previous work, we interpreted such a change in the context of a change in local viscosity due to heating, but for a tethered chromophore such an interpretation is not necessarily appropriate. For a hindered rotor, an increase in D_w indicates a reduction in the steric factors that impede it is motion. We interpret such a change in the context of a thermally induced increase of disorder in the chromophore local environment. We have reported this same phenomenon using perylene as the chromophore in lipid bilayer structures. In all cases, the average temperature change, measured by the reorientation time of the probe, was on the order of 5−15 K, depending on the system.[30,31,43] Typically, the more ordered the bath, the lower the measured transient temperature change, which is not a surprising result given the mechanism of the temperature change is vibrational energy transfer, a phenomenon that will proceed more rapidly in organized media than in disorganized media. Our data for SR-DMPE show a pronounced change in D_w upon excitation to the S_2, with typically a factor of 2 increase. For the 0.01 mol % systems, we observe no change in the confining cone angle for excitation of the two different states, but for the 0.1 mol % systems there is a substantial increase in the cone angle for S_2 excitation. This is not surprising because of the higher density of chromophores in these latter systems and the consequent opportunity to provide more points of thermal disruption per unit area of lipid layer. It is significant to note that the change in organization is most pronounced in the lipid headgroup region, no doubt due to the location of the chromophore, but for sufficiently high probe concentration the lipid acyl chain region also appears to be disrupted.

CONCLUSIONS

We have investigated the anisotropy decay dynamics of the chromophore SR-DMPE in aqueous solution and in solutions containing DMPC. The primary purpose of this work was to determine whether or not the use of tethered chromophores such as SR-DMPE could be used to evaluate changes in the local organization of lipid-containing solutions during their processing to form vesicles. The data we report here indicate that the chromophore is sensitive to its local environment but any changes in lipid organization associated with the mixing and subsequent extrusion process proceed on a length scale that is longer than the chromophore is capable of sensing. The tethered chromophore associates with lipids in DMPC solution and, presumably, the headgroup region in aggregated lipid structures is not altered substantially by the process of extrusion.

AUTHOR INFORMATION

Corresponding Author

*Phone: (517) 355 9715 x 224. Fax: (517) 353-1793. E-mail: blanchard@chemistry.msu.edu.

ACKNOWLEDGMENT

The authors are grateful to the National Science Foundation for their support of this work through Grant CHE-0808677. We thank Professor Xuefei Huang for the use of his DLS instrument.

REFERENCES

(1) Ratto, T. V.; Longo, M. L. *Biophys. J.* **2002**, *83*, 3380.
(2) Ratto, T. V.; Longo, M. L. *Langmuir* **2003**, *19*, 1788.
(3) Anderson, T. G.; McConnell, H. M. *Biophys. J.* **2001**, *81*, 2774.
(4) Benvegnu, D. J.; McConnell, H. M. *J. Phys. Chem.* **1993**, *97*, 6686.
(5) D'Onofrio, T. G.; Binns, C. W.; Muth, E. H.; Keating, C. D.; Weiss, P. S. *J. Biol. Phys.* **2002**, *28*, 605.
(6) Keller, S. L. *J. Phys.: Condens. Matter* **2002**, *14*, 4763.
(7) Keller, S. L. *Langmuir* **2003**, *19*, 1451.
(8) Keller, S. L.; McConnell, H. M. *Phys. Rev. Lett.* **1999**, *82*, 1602.
(9) Keller, S. L.; Pitcher, W. H. I.; Huestis, W. H.; McConnell, H. M. *Phys. Rev. Lett.* **1998**, *81*, 5019.
(10) Radhakrishnan, A.; McConnell, H. M. *J. Am. Chem. Soc.* **1999**, *121*, 486.
(11) Radhakrishnan, A.; McConnell, H. M. *Biophys. J.* **1999**, *77*, 1507.
(12) Radhakrishnan, A.; McConnell, H. M. *J. Phys. Chem. B* **2002**, *106*, 4755.
(13) DeWolf, C.; Leporatti, S.; Kirsch, C.; Klinger, R.; Brezesinski, G. *Chem. Phys. Lipids* **1999**, *97*, 129.
(14) Dietrich, C.; Bagatolli, L. A.; Volovyk, Z. N.; Thompson, N. L.; Levi, M.; Jacobson, K.; Gratton, E. *Biophys. J.* **2001**, *80*, 1417.
(15) Discher, B. M.; Maloney, K. M.; Grainger, D. W.; Hall, S. B. *Biophys. Chem.* **2002**, *101−102*, 333.

(16) Discher, B. M.; Maloney, K. M.; Grainger, D. W.; Sousa, C. A.; Hall, S. B. *Biochemistry* **1999**, *38*, 374.
(17) Lee, K. Y. C.; Klingler, J. F.; McConnell, H. M. *Nature* **1994**, *263*, 655.
(18) Maloney, K. M.; Grainger, D. W. *Chem. Phys. Lipids* **1993**, *65*, 31.
(19) Maloney, K. M.; Grandbois, M.; Grainger, D. W.; Salesse, C.; Lewis, K. A.; Roberts, M. F. *Biochim. Biophys. Acta* **1995**, *1235*, 395.
(20) Nag, K.; Pao, J.-S.; Harbottle, R. R.; Possmayer, F.; Peterson, N. O.; Bagatolli, L. A. *Biophys. J.* **2002**, *82*, 2041.
(21) Samsonov, A. V.; IMihalyov, I.; Cohen, F. S. *Biophys. J.* **2001**, *81*, 1486.
(22) Subramaniam, S.; McConnell, H. M. *J. Phys. Chem.* **1987**, *91*, 1715.
(23) Sugihara, G.; Yamamoto, S. K.; Nagadome, S.; Lee, S.; Sasaki, Y.; Shibata, O.; Igimi, H. *Colloids Surf., B* **1996**, *6*, 81.
(24) Conboy, J. C.; Liu, S.; O'Brien, D. F.; Saavedra, S. S. *Biomacromolecules* **2003**, *4*, 841.
(25) Anglin, T. C.; Liu, J.; Conboy, J. C. *Biophys. J.: Biophys. Lett.* **2007**, *91*, L01.
(26) Liu, J.; Conboy, J. C. *Biophys. J.* **2005**, *89*, 2522.
(27) Ross, E. E.; Bondurant, B.; Spratt, T.; Conboy, J. C.; O'Brien, D. F.; Saavedra, S. S. *Langmuir* **2001**, *17*, 2305.
(28) Ross, E. E.; Rozanski, L. J.; Spratt, T.; Liu, S. C.; O'Brien, D. F.; Saavedra, S. S. *Langmuir* **2003**, *19*, 1752.
(29) Ross, E. E.; Spratt, T.; Liu, S.; Rozanski, L. J.; O'Brien, D. F.; Saavedra, S. S. *Langmuir* **2003**, *19*, 1766.
(30) Pillman, H. A.; Blanchard, G. J. *J. Phys. Chem. B* **2010**, *114*, 13703.
(31) Pillman, H. A.; Blanchard, G. J. *J. Phys. Chem. B* **2011**, *115*, 3819.
(32) Dominska, M.; Blanchard, G. J. *Langmuir* **2010**, *26*, 1043.
(33) Greenough, K. P.; Blanchard, G. J. *J. Phys. Chem. A* **2007**, *111*, 558.
(34) Greenough, K. P.; Blanchard, G. J. *Spectrochim. Acta A* **2009**, *71*, 2050.
(35) Greiner, A. J.; Pillman, H. A.; Worden, R. M.; Blanchard, G. J.; Ofoli, R. Y. *J. Phys. Chem. B* **2009**, *113*, 13263.
(36) Koan, M. M.; Blanchard, G. J. *J. Phys. Chem. B* **2006**, *110*, 16584.
(37) Lapinski, M. M.; Castro-Forero, A.; Greiner, A. J.; Ofoli, R. Y.; Blanchard, G. J. *Langmuir* **2007**, *23*, 11677.
(38) Sternin, E.; Nizza, D.; Gawrisch, K. *Langmuir* **2001**, *17*, 2610.
(39) Rowat, A. C.; Davis, J. H. *Biochim. Biophys. Acta* **2004**, *1661*, 178.
(40) Fares, C.; Sharom, F. J.; Davis, J. H. *J. Am. Chem. Soc.* **2002**, *124*, 11232.
(41) Hughes, A. V.; Roser, S. J.; Gerstenberg, M. C.; Goldar, A.; Stidder, B.; Feidenhans'l, R.; Bradshaw, J. *Langmuir* **2002**, *18*, 8161.
(42) Hay, C. E.; Marken, F.; Blanchard, G. J. *J. Phys. Chem. A* **2010**, *114*, 4957.
(43) Dela Cruz, J. L.; Blanchard, G. J. *J. Phys. Chem. A* **2001**, *105*, 9328.
(44) Chuang, T. J.; Eisenthal, K. B. *J. Chem. Phys.* **1972**, *57*, 5094.
(45) Debye, P. *Polar Molecules*; Chemical Catalog Co.: New York, 1929.
(46) Hu, C.-M.; Zwanzig, R. *J. Chem. Phys.* **1974**, *60*, 4354.
(47) Perrin, F. *J. Phys. Rad.* **1934**, *5*, 497.
(48) Perrin, F. *J. Phys. Rad.* **1936**, *7*, 1.
(49) Edward, J. T. *J. Chem. Educ.* **1970**, *47*, 261.
(50) Lipari, G.; Szabo, A. *Biophys. J.* **1980**, *30*, 489.